Journal of The Electrochemical Society, **157** (11) P99-P105 (2010)
0013-4651/2010/157(11)/P99/7/$28.00 © The Electrochemical Society

Electrochemical Copolymerization of 3,4-Ethylenedioxythiophene and *N*-Phenylsulfonyl Pyrrole: Morphologic, Spectroscopic, Electrochemical Characterizations

Cansev Tezcan and A. Sezai Sarac[z]

Department of Chemistry, Polymer Science and Technology, Istanbul Technical University, Maslak 34469, Istanbul, Turkey

In this paper, we demonstrate the electrochemical synthesis of a copolymer of *N*-phenylsulfonyl pyrrole (PSP) with 3,4-ethylenedioxythiophene (EDOT) as thin films on single carbon fiber microelectrodes. The deposition conditions on carbon fiber and the influence of monomer concentrations on the copolymerization were shown, as well as the electrochemistry of the resulting copolymers. The inclusion of PSP in the copolymer structure was also confirmed by Fourier transform IR–attenuated total reflectance spectroscopy, where the highest low frequency capacitance (C_{LF}) was obtained for the mole fraction of PSP 0.86. Poly(EDOT-*co*-PSP) exhibits high capacitances compared to that of poly(3,4-ethylenedioxythiophene), which was shown by electrical impedance spectroscopy and equivalent circuit modeling (ECM). *n* values obtained from the ECM indicates the porosity of the electrode, which almost remains constant as ~1 for $X_{PSP} = 0.00, 0.66, 0.86$. Charge-transfer resistance (R_1) shows an increasing trend with PSP inclusion into the copolymer due to the partial destruction of conjugation. The double layer capacitance (C_{dl}) has also shown a similar behavior. Both of these parameters have exhibited an almost linear relationship with the thickness of the film. The film resistance (R_2) was between 0.88 and 10 $k\Omega\ cm^2$. According to the calculations from the ECM, the inclusion of PSP in copolymer improved the capacitance and diffusion properties.
 [DOI: 10.1149/1.3490420]

Manuscript submitted May 3, 2010; revised manuscript received August 24, 2010. Published September 25, 2010.

Conducting polymers (polythiophene, polyacetylene, polypyrrole, polyaniline, etc.) have drawn the attention of the research community in the past few years. They have successful applications in the development and construction of new advanced materials including electrochemical displays, biosensors, redox capacitors, catalysis, smart windows, antistatic coatings, electromagnetic shielding, and secondary batteries.[1-4]

Poly(3,4-ethylenedioxythiophene) (PEDOT) is one of the π-conjugated conducting polymers. In particular, PEDOT is an interesting material because of its good thermal and chemical stabilities, high electrical conductivity in the p-doped state (up to 300 S cm^{-1}),[5] and its monomer has low oxidation potential. Conducting PEDOT films have been investigated for use in supercapacitors,[6] antistatic materials,[7] electrochromic devices,[8-11] and biosensors.[12] The electropolymerization of 3,4-ethylenedioxythiophene (EDOT) is used as a method to synthesize PEDOT. Most of the existing works on the electropolymerization of EDOT and electrochemical characterization of PEDOT have been carried out in organic solutions.[9,13,14] However, aqueous solutions have also been used. The solvent, the electrode, supporting electrolyte, applied polymerization potential, and applied electropolymerization method are important elements of PEDOT film synthesis by electrochemical methods.[15] The electrical properties of PEDOT result from its polymeric structure. The electron donating oxygen atoms in three and four positions not only reduce the oxidation potential of the aromatic ring but also prevent α,β-coupling during polymerization. The ethylene bridges reduce steric distortion effects to a minimum, resulting in a highly stereoregular polymer chain guaranteeing good π-conjugation.[16]

Recently, EDOT has been combined with some typical conducting polymers with promising potential applications to produce new copolymers, i.e., EDOT with pyrrole,[17,18] *N*-methyl pyrrole,[19] thiophene,[20] bithiophene,[21] 3-methylthiophene,[22] *N*-ethyl carbazole,[23] *N*-substituted carbazole,[23] and indole.[24]

In carrying out the electrochemical polymerization (EP), the substrate is critical because the nature and the bond strength between the deposited polymer and the surface of substrate determine the physicochemical properties of the resulting polymer. Deposition of electrochemically synthesized PTh derivatives had been on noble metals such as platinum[25] and gold[26] or optically transparent electrodes such as indium tin oxide-coated glass.[22] However, uses of other substrates such as titanium[22] or stainless steel[27,28] were also reported in previous studies.

In the past years, carbon-based materials have become useful for the electrochemical applications as an electrode material. Carbon has some advantages compared to other electrode materials, i.e., processability, low cost, accessibility, and thermal and chemical stabilities.[29,30] Carbon fiber microelectrodes (CFMEs) have been used as a working microelectrode for the electropolymerization of conjugated polymeric films, functionalizing the surface of carbon fiber to improve its interfacial properties. CFMEs have unique properties such as high strength, high modulus, and low density. Electrochemical polymerization of 2,2-dimethyl-3,4-propylenedioxythiophene,[16] *N*-methyl pyrrole,[31] 1-(4-methoxyphenyl)-1 *H*-pyrrole[32,33] onto CFME have also been investigated in detail.

In this work, poly(EDOT-*co*-PSP) was electropolymerized onto CFMEs by using different initial mole fractions [$X_{PSP} = 0.66, 0.86, 0.90, 0.95$, where $X_{PSP} = n_{PSP}/(n_{PSP} + n_{EDOT})$]. The deposition conditions and influence of the monomer concentrations on the copolymerization and the electrochemical behavior were studied. Electrocoated surfaces were characterized by cyclic voltammetry (CV), electrochemical impedance spectroscopy (EIS), Fourier transfer infrared (FTIR) spectroscopy, and ultraviolet–visible (UV-vis) spectrophotometry. Scanning electron microscopy (SEM) and atomic force microscopy (AFM) were used for morphological analyses.

In summary, our contributions with this paper are to show the effect of PSP mole fractions on the electrochemical properties of resulting copolymers using a variety of characterization techniques.

Experimental

Chemicals.— EDOT (Sigma–Aldrich) and PSP monomers (Aldrich Chem. Co.) were used in the study. EPs (electrocoatings) were performed in acetonitrile (ACN, LiChrosolv Reag., Merck) containing $NaClO_4$ (Sigma) with a scan rate of 30 mV/s and 10 cycles.

Electrocopolymerizations.— Electrocopolymerizations by CV were performed using a Princeton Research potentiostat/galvanostat (model 2263) interfaced to a personal computer (PC) with a Power Suite software package. The potentiostat was also connected to a Faraday cage (BAS Cell Stand C3). A three-electrode system employing carbon fiber as a working electrode, Pt button as a counter

[z] E-mail: sarac@itu.edu.tr

electrode, and Ag button as a reference electrode (as described in the Electrode preparation section) was used.

Electrode preparations.— A carbon fiber with high strength, high modulus of elasticity, and high electric conductivity (SGL SIGRAFIL C 320B, SGL Carbon Group) containing single filaments in a roving was used as the working electrode. Fabrication of all single carbon fiber microelectrodes (SCFMEs) was carried out as follows: The single carbon fiber (SGL SIGRAFIL HM485, ~7 μm in diameter, ~4 cm long) was inserted onto a 5 cm long Teflon tape, while a 2.5 cm of the fiber was kept out. A filament of the carbon fibers with a length of 8 cm (~25 fibers) was sticked onto the single carbon fiber for providing connections and electrical conductivity. A second Teflon tape with the same length was mounted and wrapped around the composition; silver paste was used on the carbon fiber filament to improve its conductivity. A multimeter was used to test the necessary conductivity. Then SCFME, initially cleaned in acetone for 2 min and rinsed with distilled water, was dried at room temperature. The electrode area was kept constant at $\sim 2 \times 10^{-3}$ cm^2 by adjusting the dipping length (~1 cm). The button electrodes were prepared by using Ag and Pt wires in glass pipes (~4.45 mm diameter) filled with methyl methacrylate. The electrodes were then polymerized by UV light, which was inert against the electrolyte solution. The surface area of the reference and the counter electrodes were kept constant (~0.47 mm^2) during the experiments.

EIS and equivalent circuit modeling.— EIS measurements were taken at room temperature (~25°C) using a conventional three-electrode cell configuration. The electrochemical cell was connected to a potentiostat (PAR 2263) connected to a PC. An electrochemical impedance software (PowerSine) was used to carry out impedance measurements between 10 mHz and 100 kHz with an applied ac signal amplitude of 10 mV. The impedance spectra were analyzed using a ZSimpWin V3.10, an ac impedance data analysis software.

FTIR-ATR.— For spectroscopic measurements, poly(EDOT-*co*-PSP) copolymers were synthesized at a constant potential (0.8 V) using stainless steel plates with different monomer concentration ratios in a $NaClO_4$/ACN solution. Polymer films on the stainless steel plate were then removed by scratching and analyzed using a Fourier transform infrared–attenuated total reflectance (FTIR-ATR) spectrometer (Perkin-Elmer, Spectrum One, having a universal ATR attachment with a diamond and ZnSe crystal C70951). A Perkin-Elmer Spectrum software was used to carry out the FTIR-ATR measurements between 650 and 4000 cm^{-1}.

UV-vis.— Oligomers of copolymers were dissolved in the electrolyte solution during electropolymerization, resulting in colored solutions measured by a Perkin-Elmer Lambda 45 UV-vis spectrometer. A Perkin-Elmer UV Winlab software was used to carry out the UV-vis measurements between 300 and 800 nm.

SEM.— Thin films of copolymers electrocoated onto carbon fibers were analyzed by SEM on a Nano Eye desktop mini-SEM instrument(SEN-3000M). SEM analysis was performed at an accelerating voltage of 5 kV. Average values of the increase in fiber thickness were obtained from SEM images (Table I). The diameters for the fibers were calculated from an average of five to six measurements on individual fibers.

Table I. Thickness of copolymer-coated SCFMEs that were calculated from SEM and total charges (ΔQ), which were given during the electropolymerizations calculated from CV.

X_{PSP}	0.66	0.86	0.90	0.95
Thickness of copolymer coated on SCFMEs (μm)	13.8	8.5	7.05	9.2
ΔQ (mC)	25.0	22.0	11.1	26.7

AFM.— Electrocoated Thin film of copolymers on silicon wafer were analyzed by AFM using a Nanosurf EasyScan AFM with a scan head of 10 μm. The EasyScan 2 software was used for imaging functions.

Results and Discussion

Electrocopolymerization of EDOT and PSP.— Multisweep cyclic voltammograms of PSP (10 mM) in the presence of EDOT (5.0, 1.6, 1.0, and 0.5 mM) at −0.8 to 1.3 V in 0.1 M $NaClO_4$/ACN on SCFME show an increase in current density with each cycle (E_{pa} = 0.1 V, E_{pc} = 0.0 V at the 10th cycle), resulting in the formation of a thin film of conducting copolymers on SCFME at 30 mV/s scan rate and 10 cycles (see Fig. 1a-c).

The redox behavior of the resulting copolymers was investigated in the same electrolyte solution by CV. The inset plots of Fig. 1a-c present the cyclic voltammograms of poly(EDOT-*co*-PSP) in monomer-free solutions at different scan rates (25–200 mV/s), indicating a regular growth and a linear increase in peak currents (oxidation and reduction peaks). These oxidation and reduction peaks obtained in the monomer-free solutions have nearly shown the same value as the corresponding peaks obtained from the CV of electrochemical growth. The scan rate dependencies of the poly(EDOT-*co*-PSP) films are presented in Fig. 1e. Both the oxidation and reduction peaks of the copolymer films were plotted using current density values with respect to the scan rate, which is due to the formation of electroactive copolymers that are well adhered. The square root of scan rates until 10 mV^2 s^{-2} shows a linear plot; redox processes seems to be nondiffusion-limited.

Ex situ FTIR-ATR measurements of poly(EDOT-co-PSP) and PEDOT.— The inclusion of PSP into the electrocopolymerized thin film and the doping with the respective anion of the supporting electrolyte were followed by FTIR-ATR (Fig. 2 and 3). This technique allows us to assign corresponding functional groups in the resulting copolymer. For spectroscopic characterization of the poly(EDOT-*co*-PSP) films, the same mole fractions of copolymers were also prepared by chronoamperometry at 0.8 V on the stainless steel plates with the same conditions of the poly(EDOT-*co*-PSP) film formation on SCFME (Scheme 1)

The band at 1470 cm^{-1} (stretching of C=C bond) and the peak at 1276 cm^{-1} (the stretching quonidal structure of thiophene) are characteristic vibrational peaks of polythiophene. The band at 1584–1626 cm^{-1} is the C–H bending and ring puckering peak of the aromatic ring of PSP. Sulfonyl stretching at 1376 cm^{-1} becomes distinct when PSP ratio is increased in the copolymer. Further vibrations from the C–S bond in the thiophene ring can be seen at 719–784 cm^{-1}, attributed to C–S stretching. The vibrations at 1063 cm^{-1} are assigned to the stretching in the alkylenedioxy group.

In Fig. 3, the assigned peak areas were obtained from the FTIR-ATR spectra. The vibrations at 948–953 cm^{-1} are the C–H bending in the phenyl ring of PSP. By increasing the PSP ratio in the copolymer, the peak areas corresponding to PSP increased. A relationship was found between the actually incorporated mole fraction of PSP (X'_{PSP}) found from the FTIR peak ratios corresponding to the peaks of PSP/PSP + EDOT and the initial mole fraction of PSP (X_{PSP}) (Fig. 3b). This result can be considered as an evidence for the participation of PSP in the copolymer structure.

Ex situ UV-vis spectrophotometric measurements of EDOT-PSP and EDOT oligomers.— The oligomers formed in the solution with no phase separation during the electrocopolymerizations of EDOT and PSP at a constant potential onto the stainless steel plate (for the FTIR-ATR characterizations) were performed, and spectroscopic changes (color) were followed by UV-vis spectroscopy.

The ex situ UV-vis spectra were recorded in ACN for different molar ratios of EDOT-PSP co-oligomers, exhibiting peaks between 610 and 740 nm, corresponding to the possible electronic transitions of π, σ, and *n* electrons (bonding level to the antibonding state of

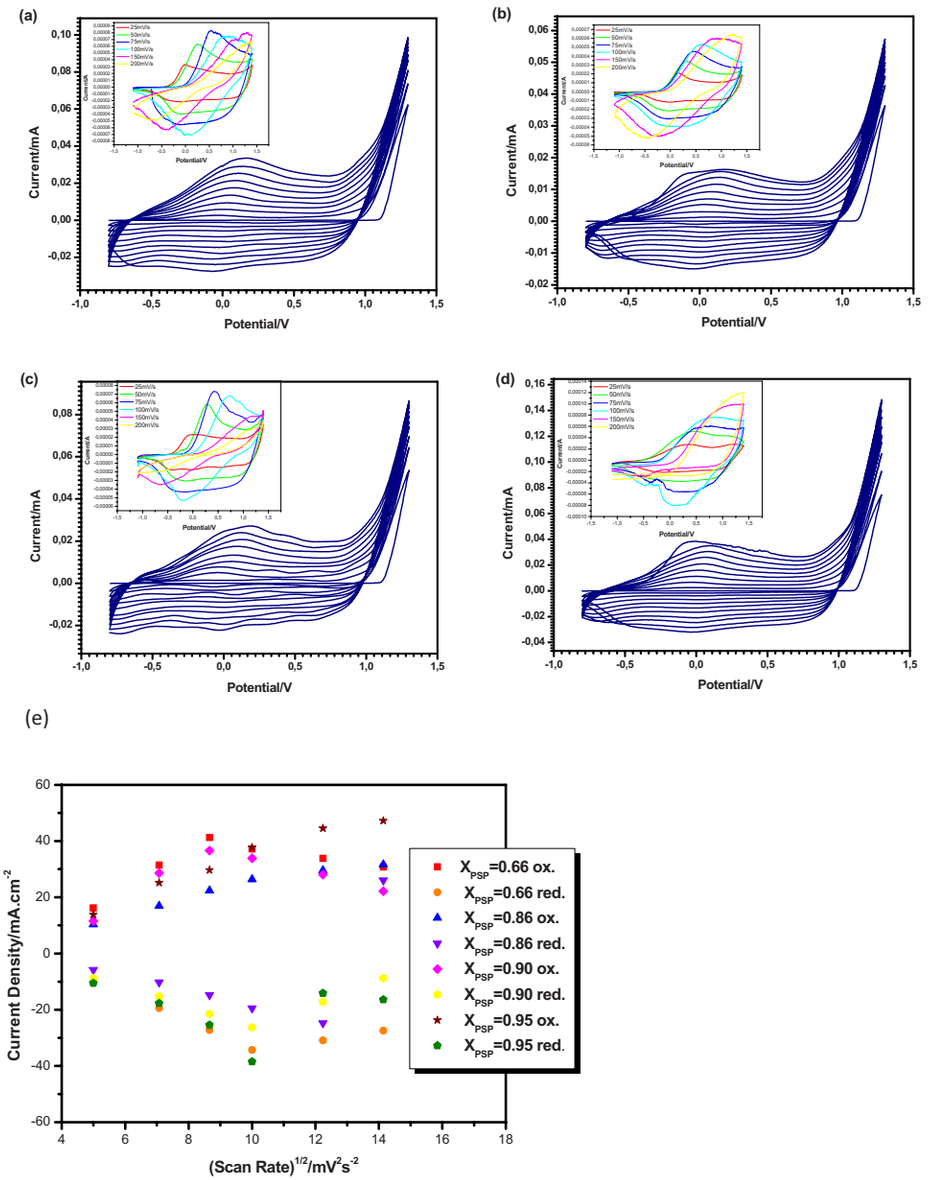

Figure 1. (Color online) CV of electrogrowth of 10 mM PSP and (a) 5 (X_{PSP} = 0.66), (b) 1.66 (X_{PSP} = 0.86), (c) 1 (X_{PSP} = 0.90), and (d) 0.5 mM (X_{PSP} = 0.95) EDOT in 0.1 M $NaClO_4$/ACN. Scan rate: 30 mV/s, scan number: 10 cycles on SCFME, and inset graphs: CV of monomer-free diagrams belongs to poly(EDOT-co-PSP) in 0.1 M $NaClO_4$/ACN at different scan rates (from 25 to 200 mV/s).(e) Anodic and corresponding cathodic peak current density vs the square root of scan rate of the poly(EDOT-*co*-PSP) films for different X_{PSP} values.

bipolaron, polaron bonding level to the π^* conduction band, and valence band to the conduction band, respectively). PSP did not polymerize under the same conditions onto the steel plate. In Fig. 4a, the absorbance of the co-oligomer peaks (possibly low molecular weight of copolymers) increases and the maximum absorption peaks shift, while the PSP ratio increases in copolymer. In the UV-vis spectrum of the EDOT oligomer measured in ACN, only one main absorption peak could be observed at 760 nm (solution color: purple). By the addition of 10 mM PSP, the peak shifted to 620 nm (solution color: blue-black) (Fig. 4b). The correlation between these changes and impedance results are under investigation.

EIS investigation and equivalent circuit modeling of poly(EDOT-co-PSP) on SCFME.— The EIS measurements were performed for different monomer concentration ratios of poly(EDOT-*co*-PSP) in the monomer-free electrolyte solution. The low frequency capacitance (C_{LF}) values from the impedance spectroscopy were obtained from the following equation using an imaginary component of impedance (Z_{IM}) corresponding to f = 0.01 Hz

$$C_{LF} = -1/2\pi f Z_{IM}$$

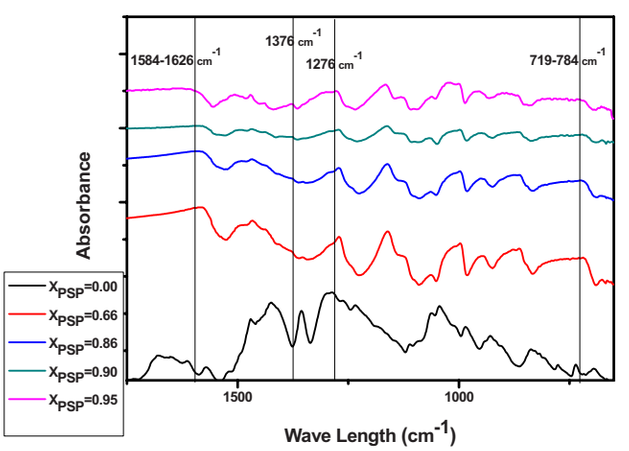

Figure 2. (Color online) Ex situ FTIR-ATR spectrum of poly(EDOT-*co*-PSP) and PEDOT powders obtained via chronoamperometry method on stainless steel plates.

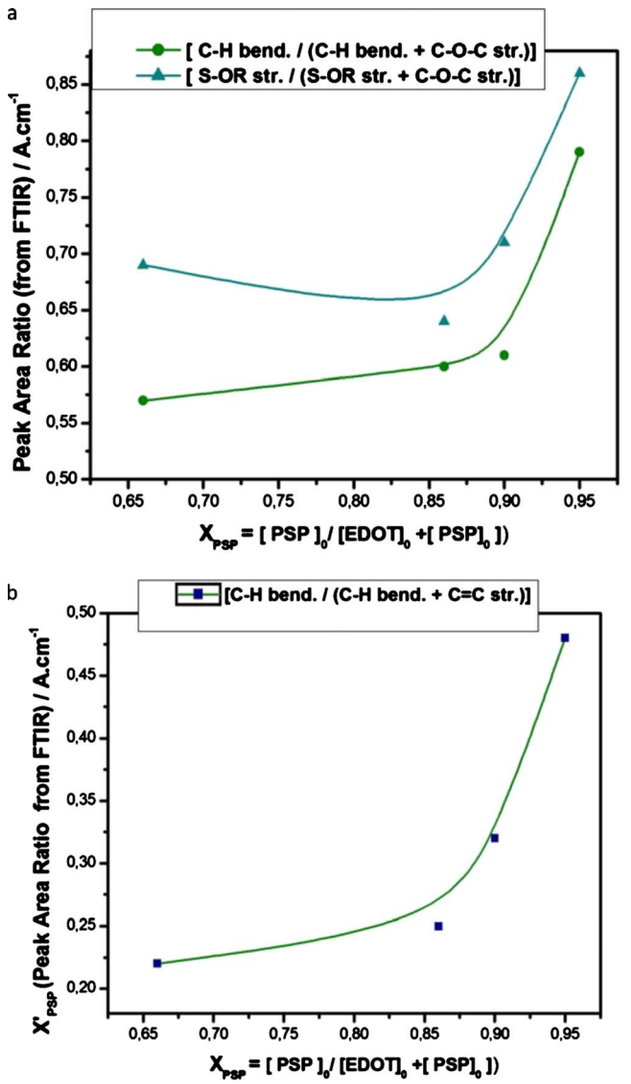

Figure 3. (Color online) (a) Comparison of FTIR-ATR peak area ratios vs initially added mole fraction of PSP (X_{PSP}). (b) Found fraction of PSP from FTIR-ATR peak area ratios with corresponding peaks of PSP taken into account vs initially added mole fraction of PSP (X_{PSP}).

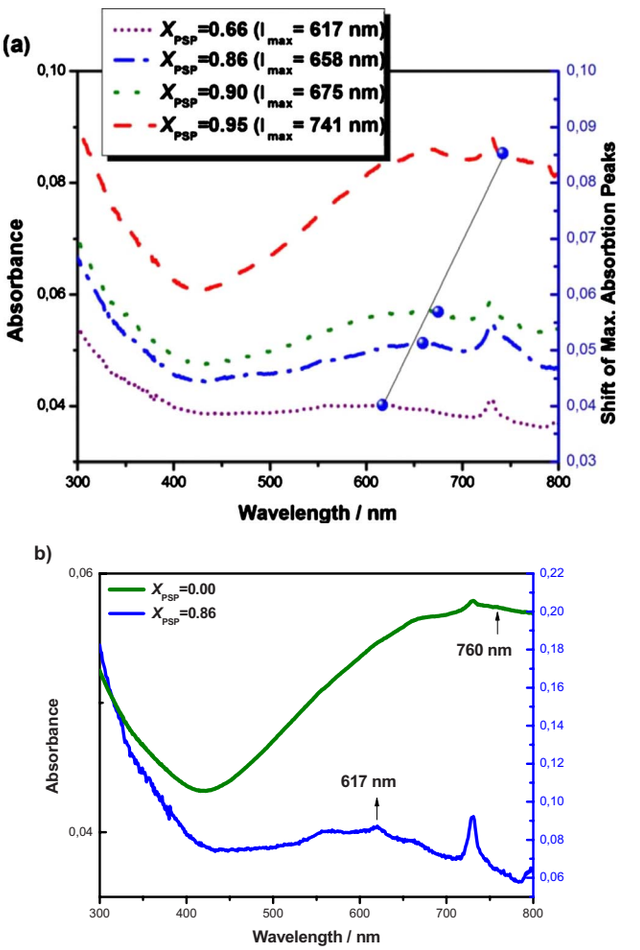

Figure 4. (Color online) Ex situ spectroelectrochemical measurements (UV-vis) of (a) different mole fractions of EDOT-PSP oligomers, (b) EDOT (X_{PSP} = 0.00), and EDOT-PSP (X_{PSP} = 0.86).

Figure 5a illustrates the Nyquist plots of the poly(EDOT-*co*-PSP) films where the magnitude of the imaginary parts are very large for all mole fractions. The system shows capacitive behavior for all values. As seen in 5d, the maximum capacitance value at low frequency (C_{LF}) was obtained for X_{PSP} = 0.86. Also, X_{PSP} = 0.95 has a semicircle plot in the Nyquist diagram indicating the smallest low frequency capacitance value. In comparison, the capacitance of the copolymers with PEDOT (X_{PSP} = 0.95) is higher than the capacitance of PEDOT as a homopolymer ($C_{LF\text{-}PEDOT}$ = 276.5 m F cm^{-2}). Figure 5b and c shows the Bode magnitude and phase angle plots at which the frequency dependence of the system is more informative compared to the Nyquist plots. The complex plane impedance plots demonstrate a vertical line with the phase angle between 58 and 80° at 0.01 Hz. The Bode phase plots also show a peak at ~1000 Hz for X_{PSP} = 0.95. The C_{LF} values increase while the film resistance values decrease by the increase in X_{PSP} (Fig. 5d). However, all the C_{LF} values of copolymers are higher than the C_{LF} value of PEDOT.

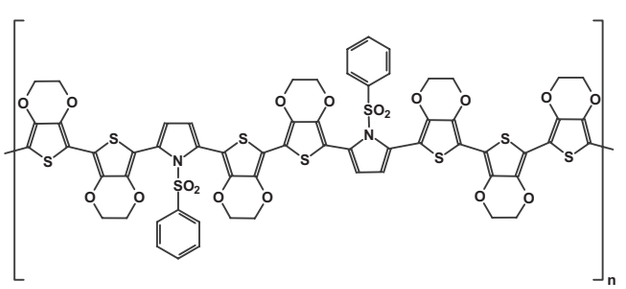

Scheme 1. Chemical structure of poly(EDOT-*co*-PSP).

The electrochemical parameters of the copolymer film in the electrolyte system ($NaClO_4$ in ACN) were evaluated by using the ZsimpWin (version 3.10) software from Princeton Applied Research. A good agreement was observed between the experimental results, the parameters obtained from the best fitting electrical equivalent circuit model, and the chi-squared (χ^2) values minimized. χ^2 is the function defined as the sum of the squares of the residuals.

An electrical equivalent circuit was used in the simulation of the impedance behavior of the film from the experimentally obtained impedance data. The proposed model (Fig. 6) was built using components in this series: The first component was the solution resistance of the polymer electrode and the electrolyte, R_s. The second one was the parallel combination of the double layer capacitance,

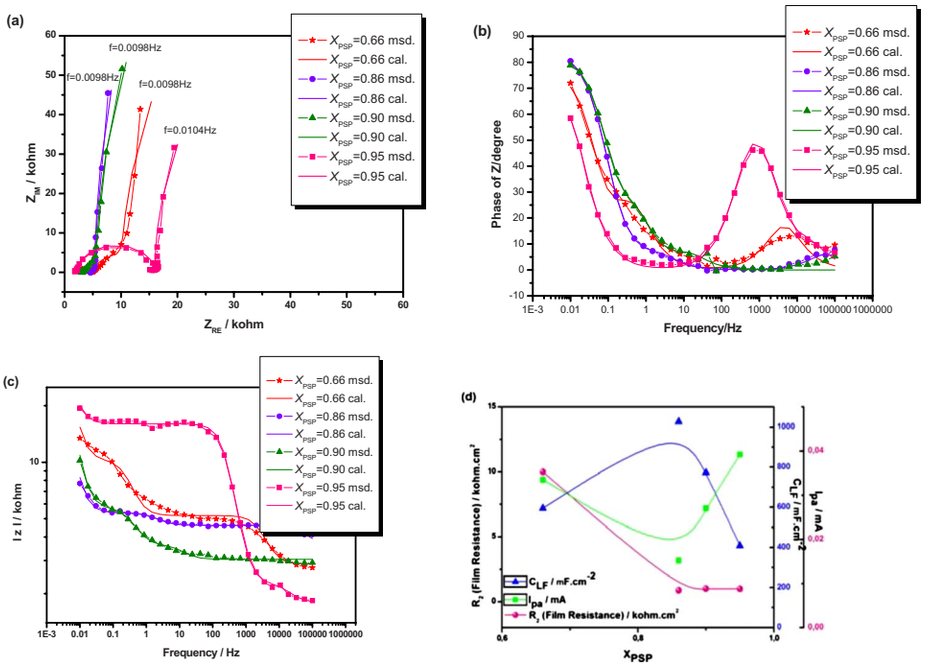

Figure 5. (Color online) (a) Nyquist, (b) Bode phase, and (c) Bode magnitude plots of poly(EDOT-*co*-PSP) electrografted on SCFMEs in 0.1 M $NaClO_4$/ACN; correlated with the calculated data from the ECM; R(C(R(Q(RW)))). (d) Low frequency capacitances, film resistances that were obtained from equivalent circuit model, and anodic peak currents that were obtained from cyclic voltammograms for different mole fractions of poly(EDOT-*co*-PSP) and PEDOT.

C_{dl}, and the charge-transfer resistance in between the polymer electrode and the electrolyte interface, R_1 (as shown in Fig. 6). The series connection to R_1 was made up using constant phase element (CPE) parallel to R_2 and W, where R_2 is the resistance of the polymer film (with a porelike morphology) and W is the Warburg impedance of diffusion of the ions in the electrolyte.

Solvent resistance (R_S) is defined as the sum of resistances due to the electrolyte on the surface or in the pores of the film and the 0.1 M $NaClO_4$/ACN solution. Solvent resistances of copolymers are lower than the solvent resistance of PEDOT as a homopolymer due to the different sizes of the pores of PEDOT and the copolymer; PEDOT has smaller pores (Fig. 7). The charge-transfer resistance (R_1) shows an increasing trend with PSP inclusion into the copolymer due to the partial destruction of conjugation. Double layer capacitance (C_{dl}) has also shown a similar behavior. Both of these parameters have exhibited an almost linear relationship with the thickness of the film. The film resistance (R_2) was between 0.88 and 10 kΩ cm^2. The variation in the film resistance could be related to the film thickness as well as to the pore distribution and sizes. However, all the copolymer films have ~1000 times lower resistance than the PEDOT film (1.9×10^4 kΩ cm^2).

CPE was used for fitting the data into the equivalent circuit, adapting to a relatively nonideal behavior. The presence of CPE can be attributed to the electrode roughness or to the inhomogeneity in the conductance or the dielectric constant.[33] The n value of CPE is regarded as a major inhomogeneity of the copolymer film ($0.72 < n < 1$). If $n = 1$, the value of an ideal capacitance can be determined from the Bode plot. From the definition, $Z_{CPE} = [Q(j\omega)^n]^{-1}$, where the parameter Q characterizes properties related to the surface and the electroactive species and ω is the angular frequency ($\omega = 2\pi f$). The exponent n arises from the slope of the log Z vs log f plot. In general, the slope of the log Z vs log f plot (denoted as n) is a manifestation of the electrode nature.[34] The n values denote the porosity of the electrode, which almost remains constant for X_{PSP}

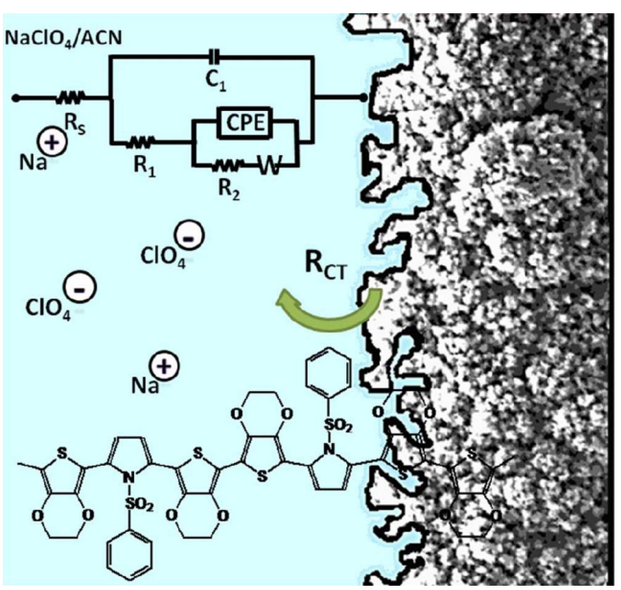

Figure 6. (Color online) Scheme of the equivalent circuit model and polymer electrolyte interface.

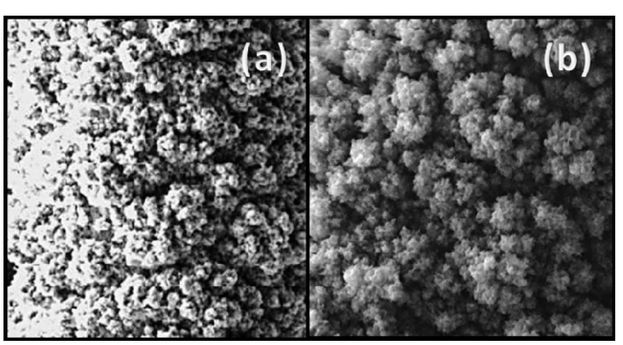

Figure 7. SEM images of (a) poly(EDOT-*co*-PSP) (scale 20 × 20 μm) and (b) PEDOT (scale 30 × 30 μm), which show the difference between pore formation.

Table II. Mole fraction dependence of parameters calculated from the ECM for PEDOT and poly(EDOT-*co*-PSP).

X_{PSP}	0.00	0.66	0.86	0.90	0.95
R_S (Ω cm^2)	16.89	7.67	6.05	3.24	7.01
C_{dl} (μF cm^{-2})	2×10^{-5}	0.056	0.052	0.072	0.109
R_1 (Ω cm^2)	2.56	3.36	5.30	3.57	7.83
CPE; Y_o (S s^{-n} cm^{-2})	0.016	5.135	0.566	0.102	0.156
n	0.97	0.99	1.00	0.72	0.86
R_2 (kΩ cm^2)	1.9×10^4	10.00	0.87	1.00	0.98
W; Y_o (μS s$^{-0.5}$ cm^{-2})	5.0×10^{-14}	3.3×10^{-7}	230	1180	8000
χ^2	2.0×10^{-3}	4.2×10^{-4}	5.2×10^{-3}	9.6×10^{-4}	5.0×10^{-3}

= 0.00,0.66,0.86. By increasing the PSP amount in the copolymer, the n values deviate from 1, so the Warburg diffusion capacitance prominences. According to the calculations from the equivalent circuit modeling (ECM), the inclusion of PSP in the copolymer improved capacitance and diffusion properties (Table II).

Morphological analyses of poly(EDOT-co-PSP) films via SEM and AFM.— Morphological analyses were made via SEM and AFM. The SEM images of poly(EDOT-*co*-PSP) copolymers obtained at 5 kV were examined and illustrated in Fig. 8. The PEDOT film has a nanostructure (pores) depending on the preparation conditions. Copolymer morphology is very similar for all mole fractions, and poly(EDOT-*co*-PSP) copolymers have larger pores as compared to PEDOT (Fig. 7). For the case examined, poly(EDOT-*co*-PSP) appears to hold a "cauliflower" shape with large sizes of pores (Fig. 8).

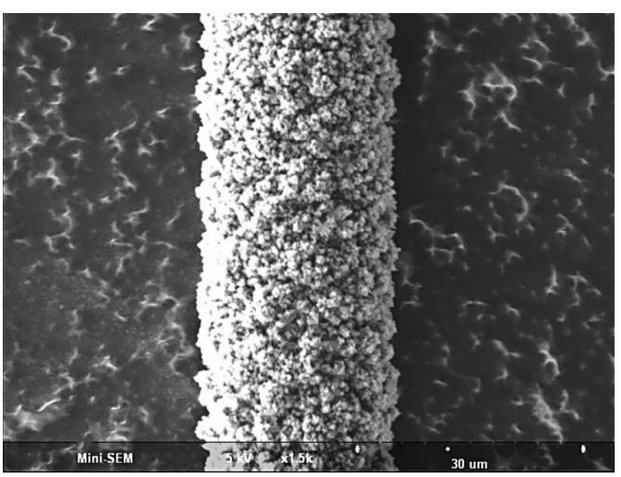

Figure 8. SEM image of the copolymer-coated SCFME with a mole fraction of PSP of 0.95.

The thicknesses of the copolymer-coated SCFMEs and total charges are shown in Table I. A correlation between the total charges applied for the polymerization and film thickness was observed for the AFM analysis of poly(EDOT-*co*-PSP) synthesized onto a boron-doped p-type silicon wafer (0.001 Ω/cm). Chronoamperometric technique was used for the EP by using 1.66 mM EDOT and 10 mM PSP (X_{PSP} = 0.86) at 0.8 V in 0.1 M $NaClO_4$/ACN electrolyte solution. A blue-black homogeneous film was obtained on the silicon wafer and washed with ACN to remove the unpolymerized monomers. The roughness analyses were performed on a smaller area on the silicon wafer. The poly(EDOT-*co*-PSP)-coated surface has 51.44 nm roughness (for 7.62 μm^2 area) with a cauliflower-like structure, which have been reported for poly[1-(4-methoxyphenyl)-1 *H*-pyrrole] in Ref. 32 (Fig. 9).

The different morphologies and thicknesses obtained with different substrates used in this study does not allow to make comparison of results, which is also reported previously where the effect of electrode substrate on the morphology and selectivity of overoxidized polypyrrole films was studied, and the substrate plays a definite role on the resulting polymer morphology by using glassy carbon and rough pyrolytic graphite.[35]

The AFM data suggest that there are different regions with different structures, particularly the bundles of fibers that seem to grow between the cauliflower aggregates, so it is not only made up of alternating EDOT and *N*-phenylsulfonyl pyrrole subunits, but there is a possibility of formation of homopolymer.

Conclusions

In this study, different mole fractions of the poly(EDOT-*co*-PSP) films were synthesized electrochemically on SCFMEs. The deposition conditions on the carbon fiber and the influence of the monomer

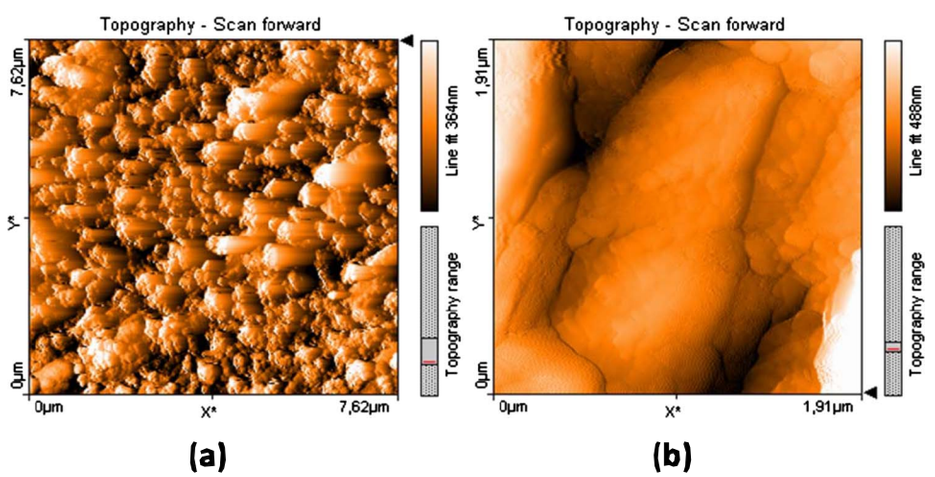

Figure 9. (Color online) AFM topographies of poly(EDOT-co-PSP)-coated silicon wafer at (a) 7.62 $\times$ 7.62 and (b) 1.91 $\times$ 1.91 μm.

concentrations on the resulting copolymer have shown higher capacitance for $X_{PSP} = 0.86$. EIS and ECM were employed to characterize the electrochemical behavior of the electrochemically prepared poly(EDOT-*co*-PSP) films in $NaClO_4$/ACN. The FTIR-ATR characteristic peaks of PSP indicate the inclusion into copolymer. The changing of the capacitance of the copolymer is reflected on the equivalent circuit model by the dependency of the mole fractions. The inclusion of PSP in the copolymer improved the capacitance and diffusion properties proved by the ECM.

Acknowledgments

This work was supported partly by the project of the Scientific and Technological Research Council of Turkey (TUBITAK) (project no. 107T933: Preparation and Characterization of Nanostructured Thin Films Based on Electrically Active Polymers).

References

1. T. A. Skotheim, R. L. Elsenbaumer, and J. R. Reynolds, *Handbook of Conducting Polymers*, Marcel Dekker, New York (1998).
2. J. D. Stenger-Smith, C. K. Webber, N. Anderson, A. P. Chafin, K. Zang, and J. R. Reynolds, *J. Electrochem. Soc.*, **149**, A973 (2002).
3. H. Randriamahazaka, V. Noël, and C. Chevrot, *J. Electroanal. Chem.*, **521**, 107 (2002).
4. G. Inzelt, M. Piner, J. W. Schultze, and M. A. Vorotyntsev, *Electrochim. Acta*, **45**, 2403 (2000).
5. A. Czardybon and M. Lapkowski, *Synth. Met.*, **119**, 161 (2001).
6. J. C. Carlberg and O. Inganäs, *J. Electrochem. Soc.*, **144**, L61 (1997).
7. F. Jonas and J. T. Morrison, *Synth. Met.*, **85**, 1397 (1997).
8. Q. B. Pei, G. Zuccarello, M. Ahlskag, and O. Inganäs, *Polymer*, **35**, 1347 (1994).
9. G. A. Sotzing, J. L. Reddinger, J. R. Reynolds, and P. J. Steel, *Synth. Met.*, **84**, 199 (1997).
10. C. Carlberg, X. W. Chen, and O. Inganäs, *Solid State Ionics*, **85**, 73 (1996).
11. J. C. Gustafsson, B. Liedberg, and O. Inganäs, *Solid State Ionics*, **69**, 145 (1994).
12. H. Yamato, M. Ohwa, and W. Wernet, *J. Electroanal. Chem.*, **397**, 163 (1995).
13. Y. Lee, S. Park, and J. Lee, *Polymer (Korea)*, **23**, 122 (1999).
14. H. Randriamahazaka, V. Noel, and C. Chevrot, *J. Electroanal. Chem.*, **472**, 103 (1999).
15. N. Sakmeche, S. Aeiyach, J. J. Aaron, M. Jouni, J. C. Lacroix, and P. C. Lacaze, *Langmuir*, **15**, 2566 (1999).
16. A. S. Sarac, H. D. Gilsing, A. Gencturk, and B. Schulz, *Prog. Org. Coat.*, **60**, 281 (2007).
17. M. Yurtsever, G. Sonmez, A. S. Sarac, *Synth. Met.*, **135/136**, 463 (2003).
18. A. S. Saraç, G. Sönmez, and F. Ç. Cebeci, *J. Appl. Electrochem.*, **33**, 295 (2003).
19. R. Oliver, A. Munoz, C. Ocampo, C. Aleman, E. Armelin, and F. Estrony, *Chem. Phys.*, **328**, 299 (2006).
20. C. C. Chang, L. J. Her, and J. L. Hong, *Electrochim. Acta*, **50**, 4461 (2005).
21. N. M. Alpatova, E. V. Ovsyannikova, F. Jonas, S. Kirmeyer, E. Y. Pisarevskoya, and M. Y. Grosheva, *Russ. J. Electrochem.*, **38**, 576 (2002).
22. T. Yohannes, J. C. Carlberg, O. Inganäs, and T. Solomon, *Synth. Met.*, **88**, 15 (1997).
23. U. Geißler, M. L. Hallensleben, and L. Toppare, *Synth. Met.*, **55**, 1483 (1993).
24. J. Xu, G. Nie, S. Zhang, X. Han, J. Hou, and S. Pu, *J. Mater. Sci.*, **40**, 2867 (2005).
25. M. A. del Valle, P. Cury, and R. Schrebler, *Electrochim. Acta*, **48**, 397 (2002).
26. A. R. Hillman and E. Mallen, *J. Electroanal. Chem. Interfacial Electrochem.*, **220**, 351 (1987).
27. H. Yamato, K. I. Kai, M. Ohwa, T. Asakuro, T. Koshiba, and W. Wernet, *Synth. Met.*, **83**, 125 (1996).
28. G. Shi, C. Li, and Y. Liang, *Adv. Mater.*, **11**, 1145 (1999).
29. E. Frackowiak and F. Beguin, *Carbon*, **39**, 937 (2001).
30. R. Kötz and M. Carlen, *Electrochim. Acta*, **45**, 2483 (2000).
31. A. S. Sarac, S. Sezgin, M. Ates, C. M. Turhan, E. A. Parlak, and B. Irfanoglu, *Prog. Org. Coat.*, **62**, 331 (2008).
32. A. Sezai Sarac, S. Sezgin, M. Ates, and M. C. Turhan, *Adv. Polym. Technol.*, **28**, 120 (2009).
33. T. C. Girija and M. V. Sangaranarayanan, *Synth. Met.*, **156**, 244 (2006).
34. H. Göhr, *Ber. Bunsenges. Phys. Chem.*, **85**, 274 (1981).
35. A. Witkowski, M. S. Freund, and A. Brajter-Toth, *Anal. Chem.*, **63**, 622 (1991).